

EXCITATIONS OF THE QUARK- GLUON PLASMA

C. M. Shakin,^{1,*} Huangsheng Wang,¹ Qing Sun,¹ Hu Li,¹ and Xiangdong Li²

¹*Department of Physics, Brooklyn College of CUNY*

Brooklyn, NY 11210, USA

²*Department of Computer System Technology,*

New York City College of Technology of CUNY, Brooklyn, NY 11201, USA

(Dated: November 2, 2004)

Abstract

We will discuss the spectrum of the eta mesons making use of the Nambu-Jona-Lasinio (NJL) model supplemented with a model of confinement. We will go on to discuss the properties of mesons at finite temperature and the phenomenon of deconfinement. We will then discuss some excited states of the quark-gluon plasma calculated in lattice QCD models. These resonances are thought to be created in heavy-ion collisions. We consider the role these states play in leading to a hydrodynamic description of the plasma at early stages of its formation.

*casbc@cunyvm.cuny.edu

I. INTRODUCTION

In this presentation we will discuss the properties of QCD as one moves upward along the temperature axis from the point at $T = 0$, where the matter density is zero. Note that for experiments at RHIC the associated chemical potential is small.

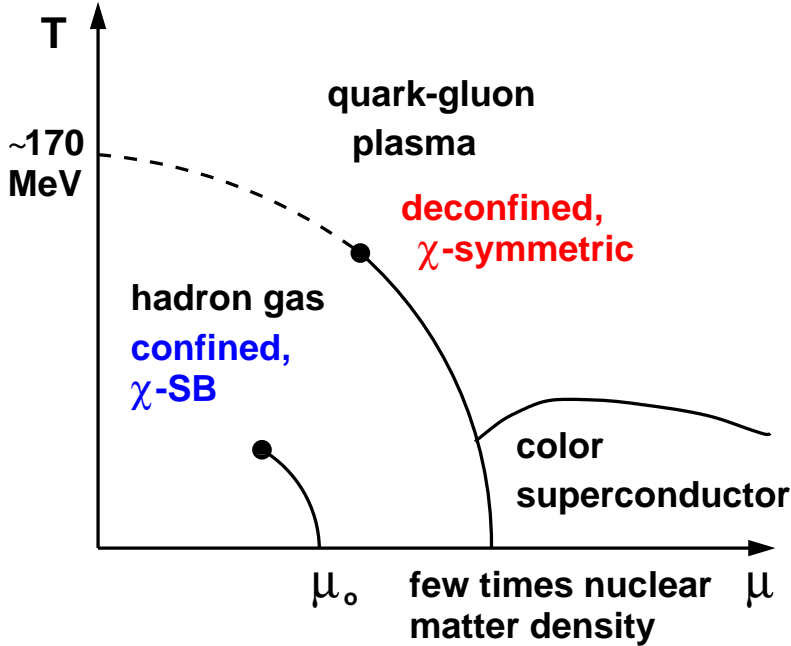




Fig. 1 Schematic phase diagram of nuclear matter (Taken from F. Karsch, Lect. Notes Phys. **583**, 209 (2002) [hep-lat/0106019].)

II. PROPERTIES OF THE η MESONS CALCULATED WITH THE NJL INTERACTION AND A MODEL OF CONFINEMENT

*C. M. Shakin and Huangsheng Wang, Physical Review D, **65**, 094003 (2002)*

Recent work has shown that the singlet-octet mixing angles of the $\eta(547)$ and $\eta'(958)$

are different. That may be demonstrated either in extended chiral perturbation theory or by analysis of a large body of experimental data. The conclusion is that the $\eta(547)$ is almost entirely of octet character, while the $\eta'(958)$ is mainly of singlet character with about 10% octet component. It is possible to calculate the mixing angles and decay constants in our generalized Nambu-Jona-Lasinio (NJL) model, which includes a covariant model of confinement. Our model is able to give a good account of the mass values of the $\eta(547)$, $\eta'(958)$, $\eta(1295)$, and $\eta(1440)$ mesons. (We also provide predictions for the mass values of a large number of radially excited states.) It is well known that the $U_A(1)$ symmetry is broken, so that we only have eight pseudo Goldstone bosons, rather than the nine we would have otherwise. In the NJL model that feature may be introduced by including the 't Hooft interaction in the Lagrangian. That interaction reduces the energy of the octet state somewhat and significantly increases the energy of the singlet state, making it possible to fit the mass values of the $\eta(547)$ and $\eta'(958)$ in the NJL model when the 't Hooft interaction is included. In this work, we derive the equations of a covariant random phase approximation that may be used to study the nonet of pseudoscalar mesons. We demonstrate that a consistent treatment of the 't Hooft interaction leads to excellent results for the singlet-octet mixing angles. (The values obtained for the singlet and octet decay constants are also quite satisfactory.) It may be seen that the difference between the up (or down) constituent quark mass and the strange quark mass induces singlet-octet mixing that is too large. However, the 't Hooft interaction contains singlet-octet coupling that enters into the theory with a sign opposite to that of the term arising from the difference of the quark mass values, leading to quite satisfactory results. In this work we present the wave function amplitudes for a number of states of the eta mesons. (The inclusion of pseudoscalar axial-vector coupling is important for our analysis and results in the need to specify eight wave function amplitudes for each state of the eta mesons.) We present the values of the various constants that parameterize our generalized NJL model and which give satisfactory values of the eta meson masses, decay constants, and mixing angles. It is found that the calculated mass values for the $\eta(1295)$ and $\eta(1440)$ are quite insensitive to variation of the parameters of the model whose values have largely been fixed in our earlier studies of other light mesons.


 G
 $-i\hat{J}(P^2)$


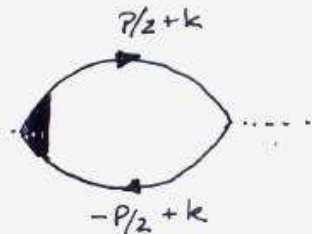
$$t = \frac{G}{1 - G\hat{J}(P^2)}$$

$$= \text{diagram 1} + \text{diagram 2} + \text{diagram 3} + \dots$$

$$t = \frac{1}{G^{-1} - \hat{J}(P^2)}$$

mass values: $G^{-1} - \hat{J}(m^2) = 0$

Confinement model:

$-iJ(P^2) = p \dots$


$$t(P^2) = \frac{1}{G^{-1} - J(P^2)}$$

$$S(p/2+k) = \frac{i}{(p/2+k) - m + i\epsilon}$$

Fig. 2

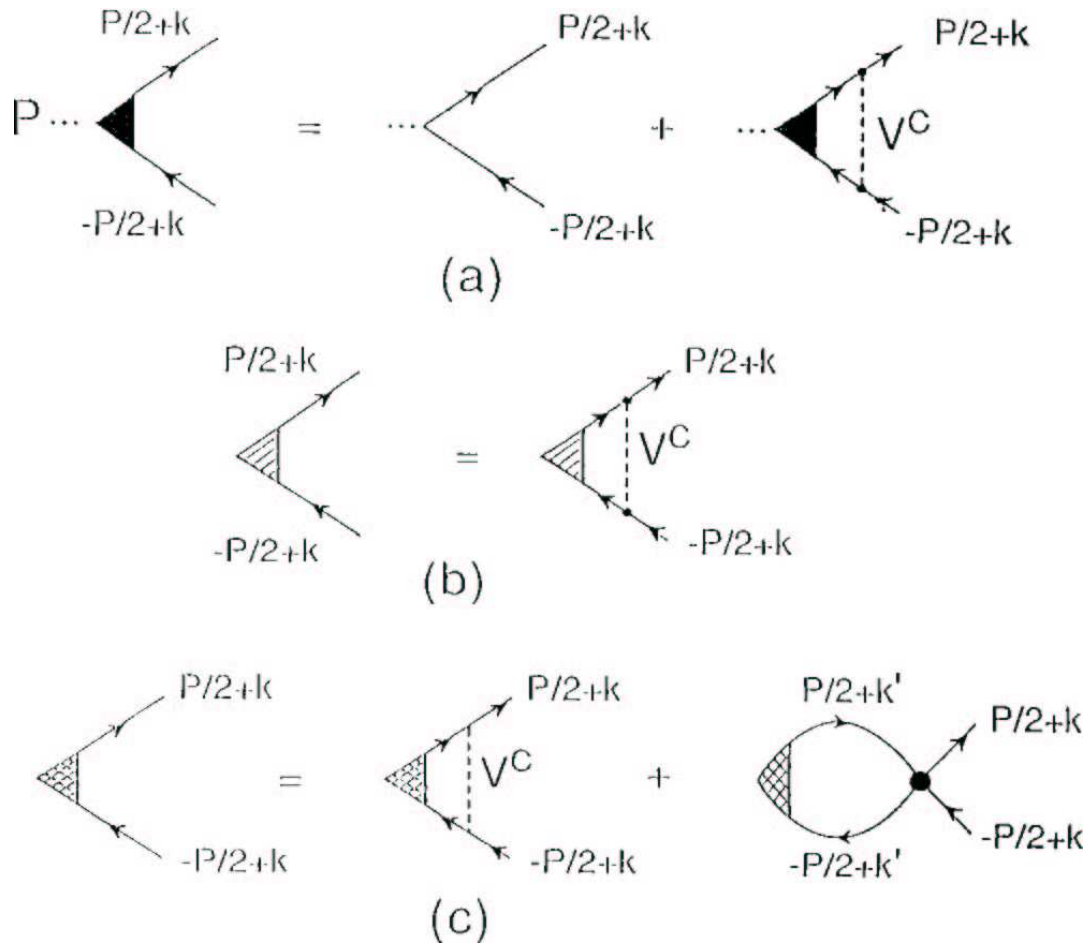


Fig. 3

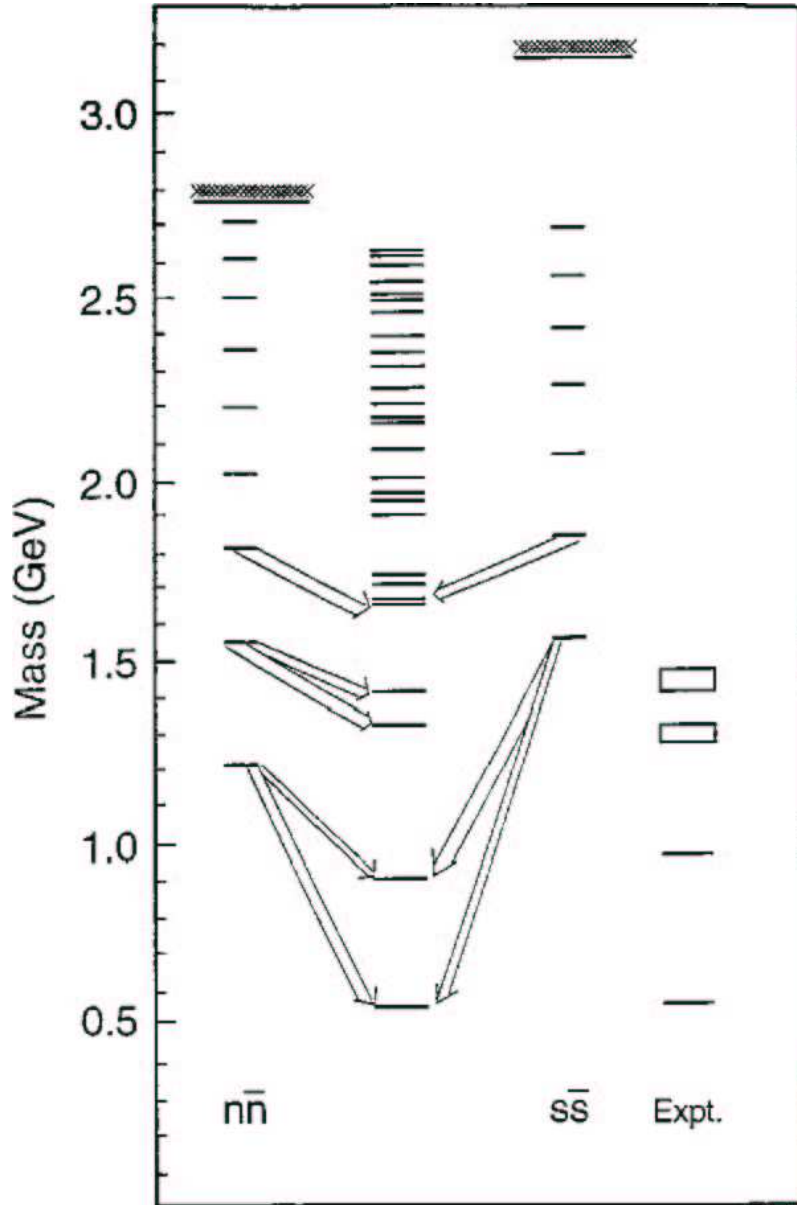


Fig. 4 Experimental and calculated spectra of the η mesons. Columns 1 and 3 show the results for the confinement potential only.

	Data	Set I	Set II	Set III	Set IV
$m_\eta(547)$ [MeV]	...	538	536	527	555
$m_{\eta'}(958)$ [MeV]	...	911	942	963	949
$m_\eta(1295)$ [MeV]	...	1319	1318	1317	1319
$m_\eta(1440)$ [MeV]	...	1414	1416	1419	1411
$\tilde{f}_\eta^{(8)}$ [MeV]	...	177.2	178.6	180.9	163
$\tilde{f}_\eta^{(0)}$ [MeV]	...	27.59	24.51	18.95	52.8
$\tilde{f}_{\eta'}^{(8)}$ [MeV]	...	-84.26	-84.64	-80.97	-105
$\tilde{f}_{\eta'}^{(0)}$ [MeV]	...	159.2	157.3	156.0	150
F_8 [MeV]	$(1.32 \pm 0.06)f_\pi$ $= 174 \pm 8$ MeV	179.3	180.3	181.9	170
F_0 [MeV]	$(1.37 \pm 0.07)f_\pi$ $= 181 \pm 9$ MeV	180.3	178.2	174.2	190
θ_η	$(-5.7 \pm 2.7)^\circ$	-8.81°	-7.82°	-6.26°	-16.1°
$\theta_{\eta'}$	$(-24.6 \pm 2.3)^\circ$	-28.0°	-28.0°	-26.4°	-38.2°
θ_0	$(-7.0 \pm 2.7)^\circ$	-9.83°	-8.76°	-6.94°	-19.4°
θ_8	$(-21.5 \pm 2.4)^\circ$	-25.4°	-25.4°	-24.1°	-32.8°
$\theta_0 - \theta_8$	16.4°	15.6°	16.6°	17.2°	13.4°
\hat{F}_0 [MeV]	$(1.21 \pm 0.07)f_\pi$ $= 160 \pm 9$ MeV	161	159	157	158
\hat{F}_8 [MeV]	$= 188 \pm 11$ MeV	196	198	198	194
G_D [GeV $^{-5}$]	...	-180	-200	-220	$-161.6(G_{08} = 0)$

III. CHIRAL SYMMETRY RESTORATION AND DECONFINEMENT OF LIGHT MESONS AT FINITE TEMPERATURE

Hu Li and C. M. Shakin , hep-ph/0209136

Confinement model:

$$V^C(r) = \kappa r \exp(-\mu_0 r), \quad (3.1)$$

$$V^C(\vec{k} - \vec{k}') = -8\pi\kappa \left[\frac{1}{[(\vec{k} - \vec{k}')^2 + \mu^2]^2} - \frac{4\mu^2}{[(\vec{k} - \vec{k}')^2 + \mu^2]^3} \right], \quad (3.2)$$

$$V^C(\hat{k} - \hat{k}') = -8\pi\kappa \left[\frac{1}{[-(\hat{k} - \hat{k}')^2 + \mu^2]^2} - \frac{4\mu^2}{[-(\hat{k} - \hat{k}')^2 + \mu^2]^3} \right], \quad (3.3)$$

$$V^C(r, T) = \kappa r \exp[-\mu(T)r], \quad (3.4)$$

$$\mu(T) = \frac{\mu_0}{1 - 0.7(T/T_c)^2}, \quad (3.5)$$

$$V_{max}(T) = \frac{\kappa[1 - 0.7(T/T_c)^2]}{\mu_0 e}. \quad (3.6)$$

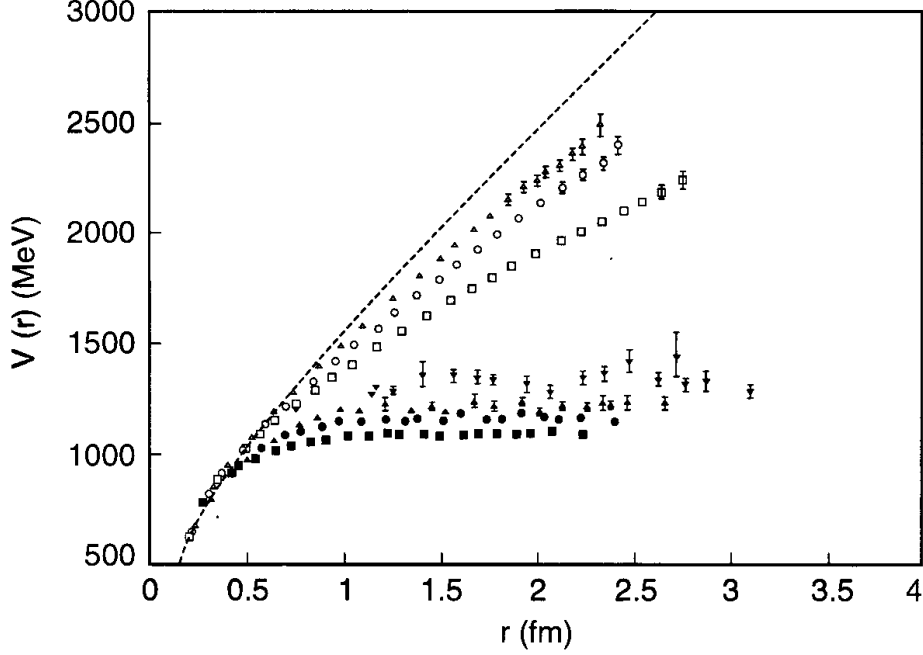


Fig. 5 A comparison of quenched (open symbols) and unquenched (filled symbols) results for the interquark potential at finite temperature. The dotted line is the zero temperature quenched potential. Here, the symbols for $T = 0.80T_c$ [open triangle], $T = 0.88T_c$ [open circle], $T = 0.94T_c$ [open square], represent the quenched results. The results with dynamical fermions are given at $T = 0.68T_c$ [solid downward-pointing triangle], $T = 0.80T_c$ [solid upward-pointing triangle], $T = 0.88T_c$ [solid circle], and $T = 0.94T_c$ [solid square].

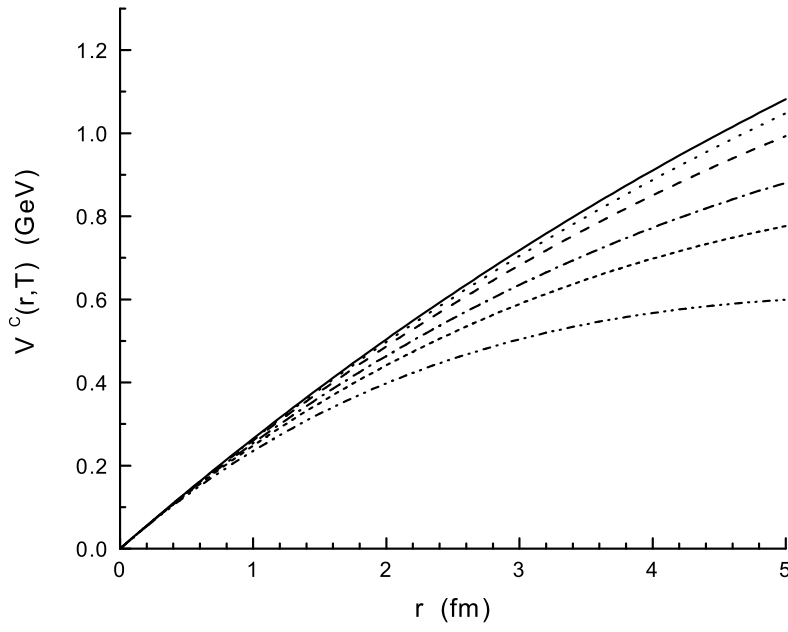


Fig. 6 The potential $V^C(r, T)$ is shown for $T/T_c = 0$ [solid line], $T/T_c = 0.4$ [dotted line], $T/T_c = 0.6$ [dashed line], $T/T_c = 0.8$ [dash-dot line], $T/T_c = 0.9$ [short dashes], $T/T_c = 1.0$ [dash-dot-dot line]. Here, $V^C(r, T) = \kappa r \exp[-\mu(T)r]$, with $\mu(T) = 0.01\text{GeV}/[1 - 0.7(T/T_c)^2]$.

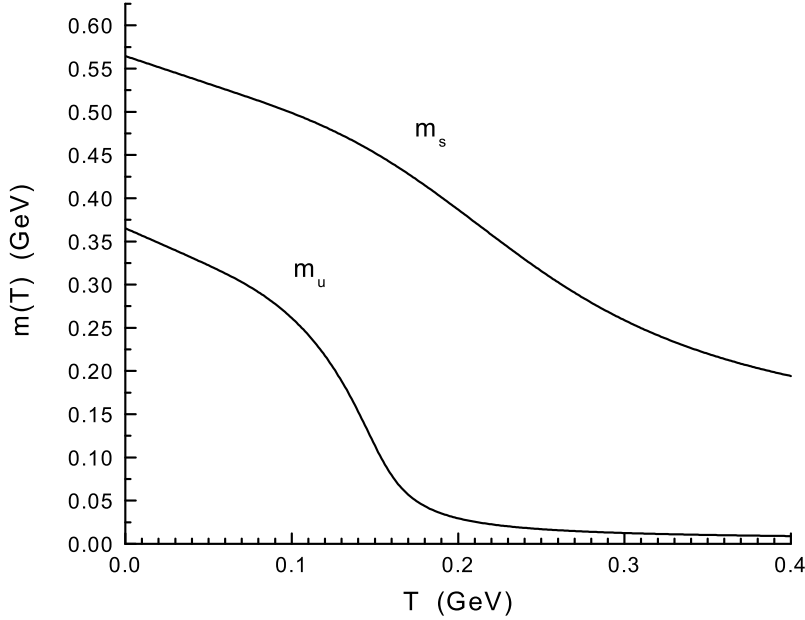


Fig. 7 Temperature dependent constituent mass values, $m_u(T)$ and $m_s(T)$, calculated using the equation below. are shown. Here $m_u^0 = 0.0055 \text{ GeV}$, $m_s^0 = 0.120 \text{ GeV}$, and $G(T) = 5.691[1 - 0.17(T/T_c)]$, if we use Klevansky's notation.

$$m(T) = m^0 + 2G_S(T)N_C \frac{m(T)}{\pi^2} \int_0^\Lambda dp \frac{p^2}{E_p} \tanh(\frac{1}{2}\beta E_p).$$

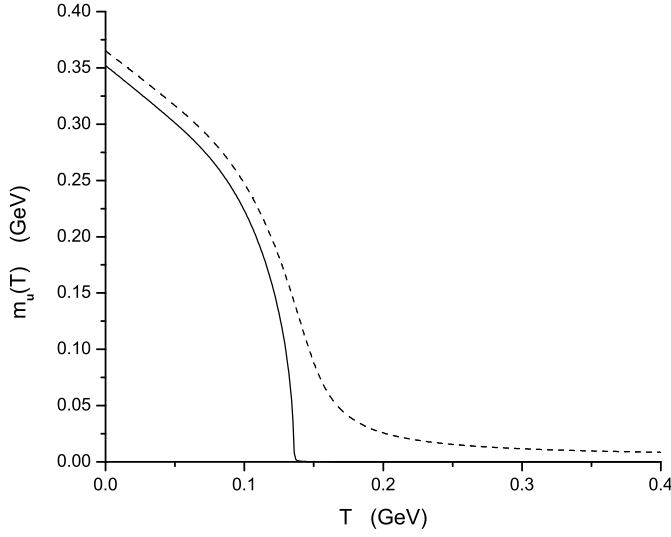


Fig. 8 Values of $m_u(T)$ are shown. The dashed curve is calculated with $m^0 = 5.50$ MeV. Here, $G(T) = G [1 - 0.17 (T/T_c)]$, with $G = 5.691 \text{ GeV}^{-2}$ and $T_c = 0.150$ GeV. The solid curve is calculated with the same value of $G(T)$ and T_c , but with $m^0 = 0$. From the solid curve, we see that chiral symmetry is restored at $T = 0.136$ GeV when $m^0 = 0$.

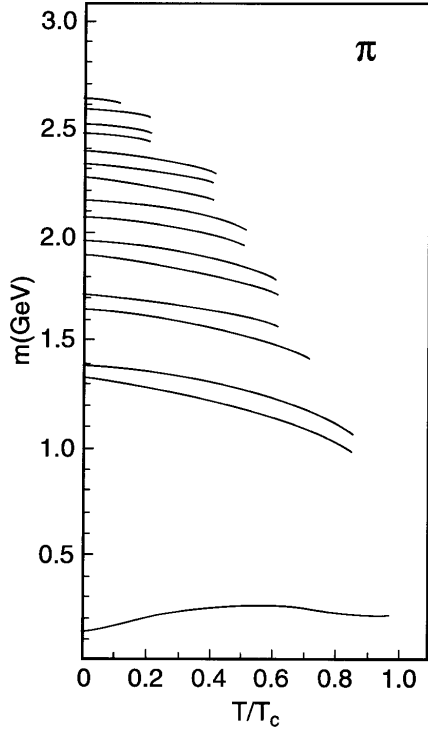


Fig. 9 The mass values of the pionic states calculated in this work with $G_\pi(T) = 13.49[1 - 0.17 T/T_c]$ GeV, $G_V(T) = 11.46[1 - 0.17 T/T_c]$ GeV. The value of the pion mass is 0.223 GeV at $T/T_c = 0.90$, where $m_u(T) = 0.102$ GeV and $m_s(T) = 0.449$ GeV. The pion is bound up to $T/T_c = 0.94$, but is absent beyond that value.

IV. CALCULATION OF HADRONIC CURRENT CORRELATION FUNCTIONS AT FINITE TEMPERATURE

*Bing He, Hu Li, C. M. Shakin, and Qing Sun, Physical Review C **67**, 065203 (2003)*

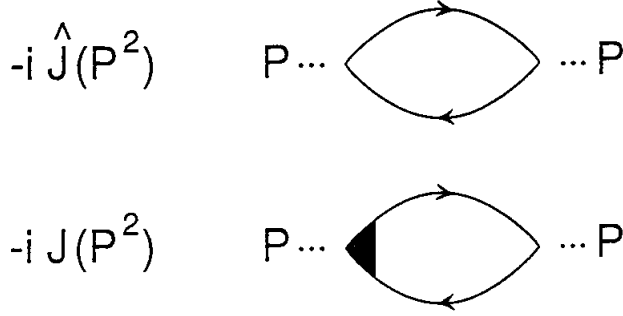


Fig. 10 The upper figure represents the basic polarization diagram of the NJL model in which the lines represent a constituent quark and a constituent antiquark. The lower figure shows a confinement vertex [filled triangular region] used in our earlier work. For the present work we neglect confinement for $T \geq 1.2 T_c$, with $T_c = 150$ MeV.

For ease of reference, we present a discussion of our calculation of hadronic current correlators. The procedure we adopt is based upon the real-time finite-temperature formalism, in which the imaginary part of the polarization function may be calculated. Then, the real part of the function is obtained using a dispersion relation. The result we need for this work has been already given in the work of Kobes and Semenoff. (The quark momentum is k and the antiquark momentum is $k - P$. We will adopt that notation in this section for ease of reference to the results presented in the work of Kobes and Semenoff.) We write the imaginary part of the scalar polarization function as

$$\begin{aligned} \text{Im } J_S(P^2, T) = & \frac{1}{2}(2N_c)\beta_S \epsilon(P^0) \int \frac{d^3k}{(2\pi)^3} e^{-\vec{k}^2/\alpha^2} \left(\frac{2\pi}{2E_1(k)2E_2(k)} \right) \\ & \{ (1 - n_1(k) - n_2(k))\delta(P^0 - E_1(k) - E_2(k)) \\ & - (n_1(k) - n_2(k))\delta(P^0 + E_1(k) - E_2(k)) \\ & - (n_2(k) - n_1(k))\delta(P^0 - E_1(k) + E_2(k)) \\ & - (1 - n_1(k) - n_2(k))\delta(P^0 + E_1(k) + E_2(k)) \} . \end{aligned} \quad (4.1)$$

Here, $E_1(k) = [\vec{k}^2 + m_1^2(T)]^{1/2}$. We have included a Gaussian regulator, $\exp[-\vec{k}^2/\alpha^2]$, with $\alpha = 0.605$ GeV, which is the same as that used in most of our applications of the NJL model in the calculation of meson properties. We also note that

$$n_1(k) = \frac{1}{e^{\beta E_1(k)} + 1}, \quad (4.2)$$

and

$$n_2(k) = \frac{1}{e^{\beta E_2(k)} + 1}. \quad (4.3)$$

For the calculation of the imaginary part of the polarization function, we may put $k^2 = m_1^2(T)$ and $(k - P)^2 = m_2^2(T)$, since in that calculation the quark and antiquark are on-mass-shell. In Eq.(4.1) the factor β_S arises from a trace involving Dirac matrices, such that

$$\beta_S = -\text{Tr}[(\not{k} + m_1)(\not{k} - \not{P} + m_2)] \quad (4.4)$$

$$= 2P^2 - 2(m_1 + m_2)^2, \quad (4.5)$$

where m_1 and m_2 depend upon temperature. In the frame where $\vec{P} = 0$, and in the case $m_1 = m_2$, we have $\beta_S = 2P_0^2(1 - 4m^2/P_0^2)$. For the scalar case, with $m_1 = m_2$, we find

$$\text{Im } J_S(P^2, T) = \frac{N_c P_0^2}{4\pi} \left(1 - \frac{4m^2(T)}{P_0^2}\right)^{3/2} e^{-\vec{k}^2/\alpha^2} [1 - 2n_1(k)], \quad (4.6)$$

where

$$\vec{k}^2 = \frac{P_0^2}{4} - m^2(T). \quad (4.7)$$

For pseudoscalar mesons, we replace β_S by

$$\beta_P = -\text{Tr}[i\gamma_5(\not{k} + m_1)i\gamma_5(\not{k} - \not{P} + m_2)] \quad (4.8)$$

$$= 2P^2 - 2(m_1 - m_2)^2, \quad (4.9)$$

which for $m_1 = m_2$ is $\beta_P = 2P_0^2$ in the frame where $\vec{P} = 0$. We find, for the π mesons,

$$\text{Im } J_P(P^2, T) = \frac{N_c P_0^2}{4\pi} \left(1 - \frac{4m^2(T)}{P_0^2}\right)^{1/2} e^{-\vec{k}^2/\alpha^2} [1 - 2n_1(k)], \quad (4.10)$$

where $\vec{k}^2 = P_0^2/4 - m_u^2(T)$, as above. Thus, we see that, relative to the scalar case, the phase space factor has an exponent of 1/2 corresponding to a s -wave amplitude. For the scalars, the exponent of the phase-space factor is 3/2.

For a study of vector mesons we consider

$$\beta_{\mu\nu}^V = \text{Tr}[\gamma_\mu(\not{k} + m_1)\gamma_\nu(\not{k} - \not{p} + m_2)], \quad (4.11)$$

and calculate

$$g^{\mu\nu}\beta_{\mu\nu}^V = 4[P^2 - m_1^2 - m_2^2 + 4m_1m_2], \quad (4.12)$$

which, in the equal-mass case, is equal to $4P_0^2 + 8m^2(T)$, when $m_1 = m_2$ and $\vec{P} = 0$. This result will be needed when we calculate the correlator of vector currents in the next section. Note that, for the elevated temperatures considered in this work, $m_u(T) = m_d(T)$ is quite small, so that $4P_0^2 + 8m_u^2(T)$ can be approximated by $4P_0^2$, when we consider the vector current correlation functions. In that case, we have

$$\text{Im } J_V(P^2, T) \simeq \frac{2}{3} \text{Im } J_P(P^2, T). \quad (4.13)$$

At this point it is useful to define functions that do not contain that Gaussian regulator:

$$\text{Im } \tilde{J}_P(P^2, T) = \frac{N_c P_0^2}{4\pi} \left(1 - \frac{4m^2(T)}{P_0^2}\right)^{1/2} [1 - 2n_1(k)], \quad (4.14)$$

and

$$\text{Im } \tilde{J}_V(P^2, T) = \frac{2}{3} \frac{N_c P_0^2}{4\pi} \left(1 - \frac{4m^2(T)}{P_0^2}\right)^{1/2} [1 - 2n_1(k)], \quad (4.15)$$

We need to use a twice-subtracted dispersion relation to obtain $\text{Re } \tilde{J}_P(P^2, T)$, or $\text{Re } \tilde{J}_V(P^2, T)$. For example,

$$\begin{aligned} \text{Re } \tilde{J}_P(P^2, T) &= \text{Re } \tilde{J}_P(0, T) + \frac{P^2}{P_0^2} [\text{Re } \tilde{J}_P(P_0^2, T) - \text{Re } \tilde{J}_P(0, T)] + \\ &\quad \frac{P^2(P^2 - P_0^2)}{\pi} \int_{4m^2(T)}^{\tilde{\Lambda}^2} ds \frac{\text{Im } \tilde{J}_P(s, T)}{s(P^2 - s)(P_0^2 - s)}, \end{aligned} \quad (4.16)$$

where $\tilde{\Lambda}^2$ can be quite large, since the integral over the imaginary part of the polarization function is now convergent. We may introduce $\tilde{J}_P(P^2, T)$ and $\tilde{J}_V(P^2, T)$ as complex functions, since we now have both the real and imaginary parts of these functions. We note that the construction of either $\text{Re } J_P(P^2, T)$, or $\text{Re } J_V(P^2, T)$, by means of a dispersion relation does not require a subtraction. We use these functions to define the complex functions $J_P(P^2, T)$ and $J_V(P^2, T)$.

In order to make use of Eq. (4.16), we need to specify $\tilde{J}_P(0)$ and $\tilde{J}_P(P_0^2)$. We found it useful to take $P_0^2 = -1.0 \text{ GeV}^2$ and to put $\tilde{J}_P(0) = J_P(0)$ and $\tilde{J}_P(P_0^2) = J_P(P_0^2)$. The quantities $\tilde{J}_V(0)$ and $\tilde{J}_V(P_0^2)$ are determined in an analogous function. This procedure in which we fix the behavior of a function such as $\text{Re}\tilde{J}_V(P^2)$ or $\text{Re}\tilde{J}_V(P^2)$ is quite analogous to the procedure used in our earlier work. In that work we made use of dispersion relations to construct a continuous vector-isovector current correlation function which had the correct perturbative behavior for large $P^2 \rightarrow -\infty$ and also described that low-energy resonance present in the correlator due to the excitation of the ρ meson. In our earlier work the NJL model was shown to provide a quite satisfactory description of the low-energy resonant behavior of the vector-isovector correlation function.

We now consider the calculation of temperature-dependent hadronic current correlation functions. The general form of the correlator is a transform of a time-ordered product of currents,

$$iC(P^2, T) = \int d^4x e^{iP \cdot x} \ll T(j(x)j(0)) \gg, \quad (4.17)$$

where the double bracket is a reminder that we are considering the finite temperature case.

For the study of pseudoscalar states, we may consider currents of the form $j_{P,i}(x) = \tilde{q}(x)i\gamma_5\lambda^i q(x)$, where, in the case of the π mesons, $i = 1, 2$ and 3 . For the study of scalar-isoscalar mesons, we introduce $j_{S,i}(x) = \tilde{q}(x)\lambda^i q(x)$, where $i = 0$ for the flavor-singlet current and $i = 8$ for the flavor-octet current.

In the case of the pseudoscalar-isovector mesons, the correlator may be expressed in terms of the basic vacuum polarization function of the NJL model, $J_P(P^2, T)$. Thus,

$$C_P(P^2, T) = \tilde{J}_P(P^2, T) \frac{1}{1 - G_P(T)J_P(P^2, T)}, \quad (4.18)$$

where $G_P(T)$ is the coupling constant appropriate for our study of π mesons. We have found $G_P(T) = 13.49 \text{ GeV}^{-2}$ by fitting the pion mass in a calculation made at $T = 0$, with $m_u = m_d = 0.364 \text{ GeV}$. The result given in Eq. (4.18) is only expected to be useful for small P^2 , since the Gaussian regulator strongly modifies the large P^2 behavior. Therefore, we suggest that the following form is useful, if we are to consider the larger values of P^2 .

$$\frac{C_P(P^2, T)}{P^2} = \left[\frac{\tilde{J}_P(P^2, T)}{P^2} \right] \frac{1}{1 - G_P(T)J_P(P^2, T)}. \quad (4.19)$$

(As usual, we put $\vec{P} = 0$.) This form has two important features. At large P_0^2 , $\text{Im } C_P(P_0, T)/P_0^2$ is a constant, since $\text{Im } \tilde{J}_P(P_0^2, T)$ is proportional to P_0^2 . Further, the denominator of Eq. (4.19) goes to 1 for large P_0^2 . On the other hand, at small P_0^2 , the denominator is capable of describing resonant enhancement of the correlation function. As we will see, the results obtained when Eq. (4.19) is used appear quite satisfactory.

For a study of the vector-isovector correlators, we introduce conserved vector currents $j_{\mu,i}(x) = \tilde{q}(x)\gamma_\mu\lambda_i q(x)$ with $i=1, 2$ and 3 . In this case we define

$$J_V^{\mu\nu}(P^2, T) = \left(g^{\mu\nu} - \frac{P^\mu P^\nu}{P^2} \right) J_V(P^2, T) \quad (4.20)$$

and

$$C_V^{\mu\nu}(P^2, T) = \left(g^{\mu\nu} - \frac{P^\mu P^\nu}{P^2} \right) C_V(P^2, T), \quad (4.21)$$

taking into account the fact that the current $j_{\mu,i}(x)$ is conserved. (Note that Eqs. (4.20) and (4.21) are valid for zero temperature. However, we still use that form at finite temperature for convenience.) We may then use the fact that

$$J_V(P^2, T) = \frac{1}{3} g_{\mu\nu} J_V^{\mu\nu}(P^2, T) \quad (4.22)$$

and

$$\text{Im } J_V(P^2, T) = \frac{2}{3} \left[\frac{P_0^2 + 2m_u^2(T)}{4\pi} \right] \left(1 - \frac{4m_u^2(T)}{P_0^2} \right)^{1/2} e^{-\vec{k}^2/\alpha^2} [1 - 2n_1(k)] \quad (4.23)$$

$$\simeq \frac{2}{3} \text{Im } J_P(P^2, T). \quad (4.24)$$

(See Eq. (4.7) for the specification of $k = |\vec{k}|$.) We then have

$$C_V(P^2, T) = \tilde{J}_V(P^2, T) \frac{1}{1 - G_V(T) J_V(P^2, T)}, \quad (4.25)$$

where we have introduced

$$\text{Im } \tilde{J}_V(P^2, T) = \frac{2}{3} \left[\frac{P_0^2 + 2m_u^2(T)}{4\pi} \right] \left(1 - \frac{4m_u^2(T)}{P_0^2} \right)^{1/2} [1 - 2n_1(k)] \quad (4.26)$$

$$\simeq \frac{2}{3} \text{Im } \tilde{J}_P(P^2, T). \quad (4.27)$$

In the literature, ω is used instead of P_0 . We may define the spectral functions

$$\sigma_V(\omega, T) = \frac{1}{\pi} \text{Im } C_V(\omega, T), \quad (4.28)$$

and

$$\sigma_P(\omega, T) = \frac{1}{\pi} \text{Im } C_P(\omega, T), \quad (4.29)$$

Since different conventions are used in the literature, we may use the notation $\bar{\sigma}_P(\omega, T)$ and $\bar{\sigma}_V(\omega, T)$ for the spectral functions given there. We have the following relations:

$$\bar{\sigma}_P(\omega, T) = \sigma_P(\omega, T), \quad (4.30)$$

and

$$\frac{\bar{\sigma}_V(\omega, T)}{2} = \frac{3}{4} \sigma_V(\omega, T), \quad (4.31)$$

where the factor 3/4 arises because there is a division by 4 in the literatures, while we have divided by 3.

V. CALCULATION OF THE MOMENTUM DEPENDENCE OF HADRONIC CURRENT CORRELATION FUNCTIONS AT FINITE TEMPERATURE

Xiangdong Li, Hu Li, C. M. Shakin, Qing Sun and Huangsheng Wang, nucl-th/0405081

We have calculated spectral functions associated with hadronic current correlation functions for vector currents at finite temperature. We made use of a model with chiral symmetry, temperature-dependent coupling constants and temperature-dependent momentum cutoff parameters. Our model has two parameters which are used to fix the magnitude and position of the large peak seen in the spectral functions. In our earlier work, good fits were obtained for the spectral functions that were extracted from lattice data by means of the maximum entropy method (MEM). In the present work we extend our calculations and provide values for the three-momentum dependence of the vector correlation function at $T = 1.5 T_c$. These results are used to obtain the correlation function in coordinate space, which is usually parametrized in terms of a screening mass. Our results for the three-momentum dependence of the spectral functions are similar to those found in a recent lattice QCD calculation for charmonium [S. Datta, F. Karsch, P. Petreczky and I. Wetzorke, hep-lat/0312037]. For a limited range we find the exponential behavior in coordinate

space that is usually obtained for the spectral function for $T > T_c$ and which allows for the definition of a screening mass.

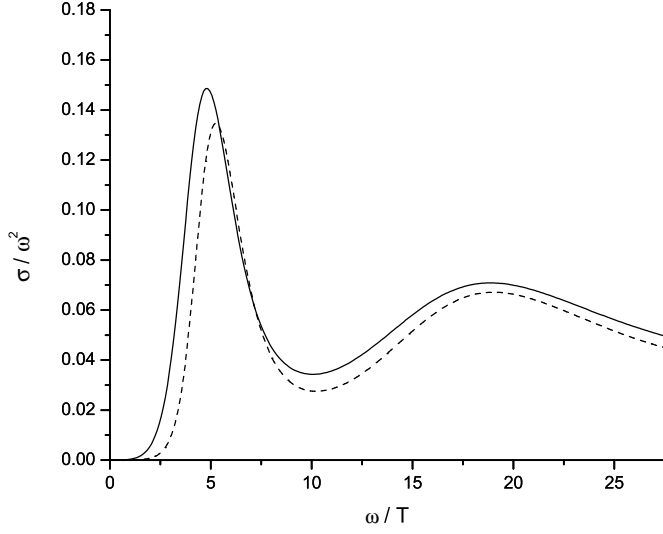


Fig. 11 The spectral functions σ/ω^2 for pseudoscalar states obtained by MEM are shown. The solid line is for $T/T_c = 1.5$ and the dashed line is for $T/T_c = 3.0$. The second peak is a lattice artifact.

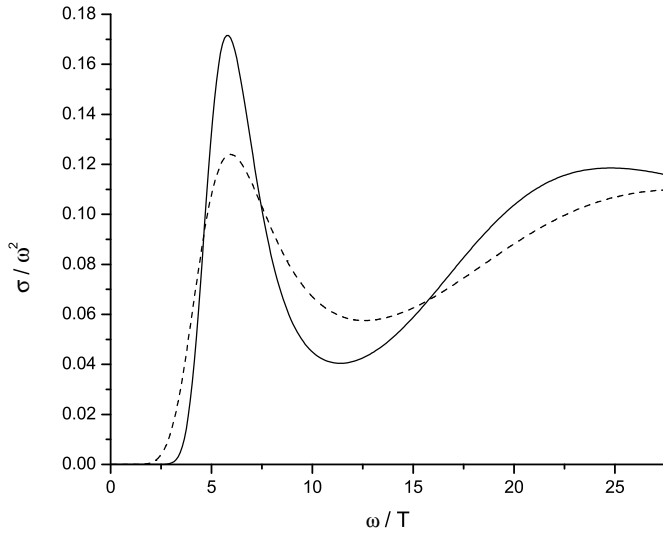


Fig. 12 The spectral functions σ/ω^2 for vector states obtained by MEM are shown. The second peak is a lattice artifact.

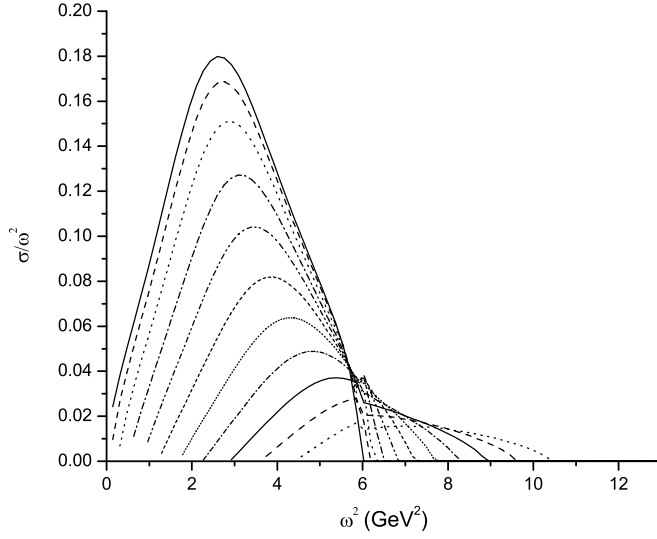


Fig. 13 The imaginary part of the correlator $\sigma(\omega)/\omega^2$ is shown for various values of $|\vec{P}|$ as a function of ω^2 . Starting with the topmost curve the values of $|\vec{P}|$ in GeV units are 0.10, 0.30, 0.50, 0.70, 0.90, 1.10, 1.30, 1.50, 1.70, 1.90 and 2.10. Here we have used $G_S = 1.2$ GeV $^{-2}$ and $k_{max} = 1.22$ GeV.

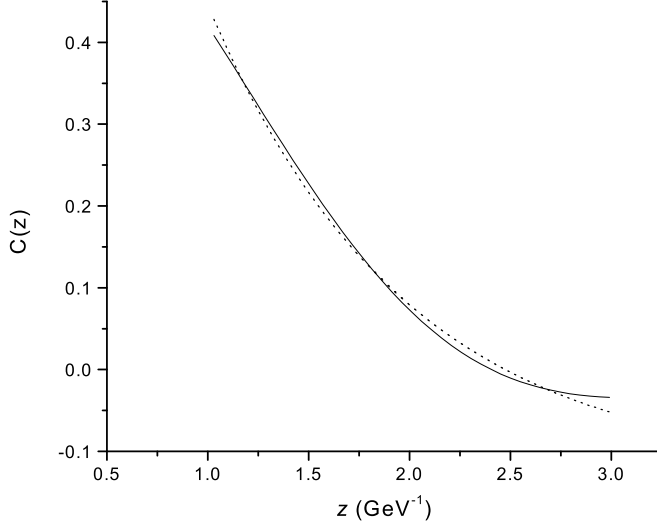


Fig. 14 The correlation function $C(z)$ is shown. The dotted line represents a fit using an exponential function.

Here, $C(z) = \frac{1}{2} \int_{-\infty}^{\infty} dP_z e^{iP_z z} \int_0^{\infty} d\omega \frac{\sigma(\omega, 0, 0, P_z)}{\omega}$. We may also use the form $C(z) = \frac{1}{4} \int_{-\infty}^{\infty} dP_z e^{iP_z z} \int_0^{\infty} dP^2 \frac{\sigma(P^2, 0, 0, P_z)}{P^2}$.

VI. QUARK PROPAGATION IN THE QUARK-GLUON PLASMA

*Xiangdong Li, Hu Li, C. M. Shakin and Qing Sun, Physical Review C, **69**, 065201 (2004)*

It has recently been suggested that the quark-gluon plasma formed in heavy-ion collisions behaves as a nearly ideal fluid. That behavior may be understood if the quark and antiquark mean-free- paths are very small in the system, leading to a “sticky molasses” description of the plasma, as advocated by the Stony Brook group. This behavior may be traced to the fact that there are relatively low-energy $q\bar{q}$ resonance states in the plasma leading to very large scattering lengths for the quarks. These resonances have been found in lattice simulation of QCD using the maximum entropy method (MEM). We have used a chiral quark model, which provides a simple representation of effects due to instanton dynamics, to study the resonances obtained using the MEM scheme. In the present work we use our model to study the optical potential of a quark in the quark-gluon plasma and calculate the quark mean-free-path. Our results represent a specific example of the dynamics of the plasma as described by the Stony Brook group.

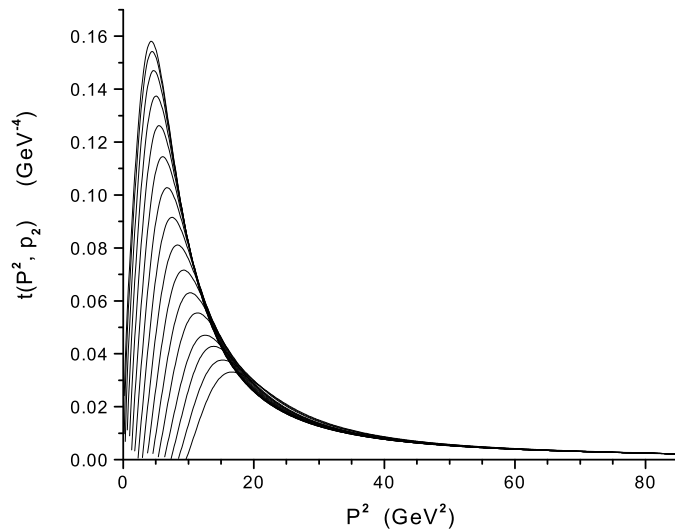


Fig. 15 Values of $t(P^2, p_2)$ are shown for various values of the quark momentum $|\vec{p}_2|$. Starting with the uppermost curve, the $|\vec{p}_2|$ values in GeV units are 0.01, 0.03, 0.05, 0.07,

0.09, 0.11, 0.13, 0.15, 0.17, 0.19, 0.21, 0.23, 0.25, 0.27, 0.29 and 0.31. (For large P^2 , we have $t(P^2, p_2) \simeq (1/\pi P^2)G$.) Here $P^2 = (p_1 + p_2)^2$, where p_1 is the antiquark momentum.

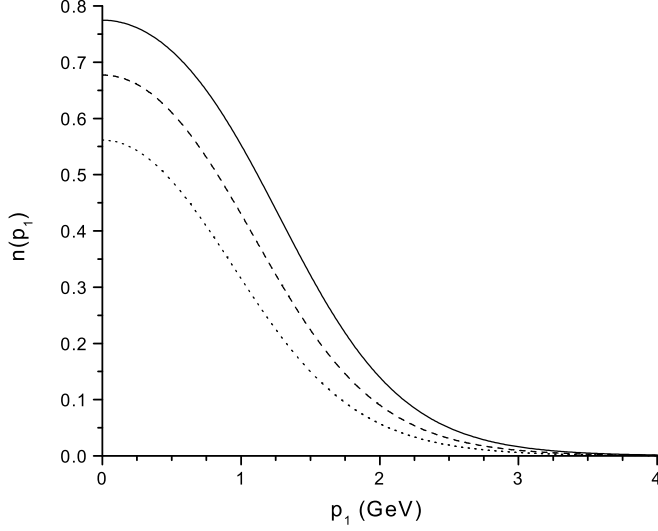


Fig. 16 Values of $n(p_1)$ are shown for $\mu = 1.1$ GeV (dotted curve), $\mu = 1.3$ GeV (dashed curve) and $\mu = 1.5$ GeV (solid curve). Here $T = 1.5 T_c$ with $T_c = 270$ MeV.

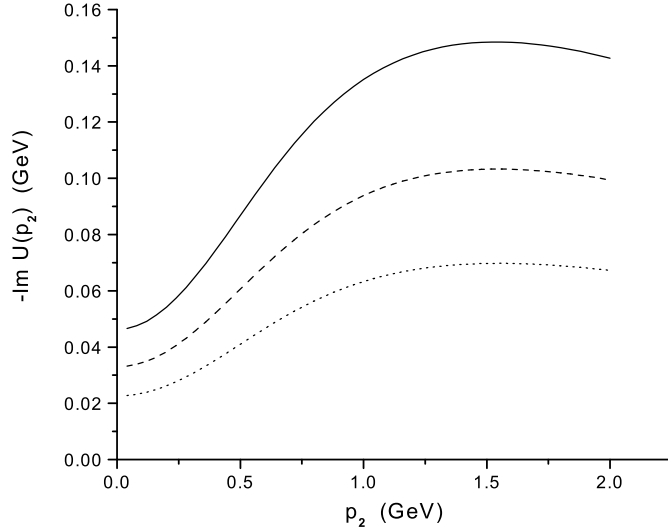


Fig. 17 The imaginary part of the quark optical potential is shown for $\mu = 1.1$ GeV (dotted curve), $\mu = 1.3$ GeV (dashed curve) and $\mu = 1.5$ GeV (solid curve). (We recall that the nucleon-nucleus imaginary optical potential is about 0.01 GeV in magnitude.)

VII. CALCULATION OF SCREENING MASSES IN A CHIRAL QUARK MODEL

Xiangdong Li, Hu Li, C. M. Shakin and Qing Sun, nucl-th/0405035

We consider a simple model for the coordinate-space vacuum polarization function which is often parametrized in terms of a screening mass. We discuss the circumstances in which the value $m_{sc} = \pi T$ is obtained for the screening mass. In the model considered here, that result is obtained when the momenta in the relevant vacuum polarization integral are small with respect to the first Matsubara frequency.

In order to present our results in the simplest form, we consider only the scalar interaction proportional to $(\bar{q}q)^2$. We also extend the definition of $\sigma(\omega, T)$ to include a dependence upon the total moment of the quark and antiquark appearing in the polarization integral. Thus we consider the imaginary part of the correlator, $\sigma(\omega, \vec{P})$. Since we place \vec{P} along the z -axis this quantity may be written as $\sigma(\omega, 0, 0, P_z)$. In this work we will present our result for the coordinate-dependent correlator $C(z)$ which is proportional to the correlator,

$$C(z) = \frac{1}{2} \int_{-\infty}^{\infty} dP_z e^{iP_z z} \int_0^{\infty} d\omega \frac{\sigma(\omega, 0, 0, P_z)}{\omega}. \quad (7.1)$$

We may also use the form

$$C(z) = \frac{1}{4} \int_{-\infty}^{\infty} dP_z e^{iP_z z} \int_0^{\infty} dP^2 \frac{\sigma(P^2, 0, 0, P_z)}{P^2}. \quad (7.2)$$

We have made a study of the screening mass in a simple model in order to understand the origin of exponential behavior for the correlator. We consider the Matsubara formalism and note that the quark propagator may be written, with $\beta = 1/T$,

$$S_\beta(\vec{k}, \omega_n) = \frac{\gamma^0(2n+1)\pi/\beta + \vec{\gamma} \cdot \vec{k} - M}{(2n+1)^2\pi^2/\beta^2 + \vec{k}^2 + M^2}. \quad (7.3)$$

For bosons the vacuum polarization function is given as,

$$\Pi(\vec{p}, p^0) = \frac{g^2}{2\beta} \sum_n \frac{d^3k}{(2\pi)^3} \frac{1}{\frac{4n^2\pi^2}{\beta^2} + \vec{k}^2 + M^2} \cdot \frac{1}{\left(\frac{2n\pi}{\beta} + p^0\right)^2 + (\vec{k} + \vec{p})^2 + M^2}. \quad (7.4)$$

We modify the last equation to refer to fermions. In this case the Matsubara frequencies are

$$\omega_n = \frac{(2n+1)\pi}{\beta} \quad (7.5)$$

and we have

$$\Pi(\vec{p}, p^0) = \frac{g^2}{2\beta} \text{Tr} \int \frac{d^3k}{(2\pi)^3} \frac{\left[\left(\gamma^0 \pi / \beta + \vec{\gamma} \cdot \vec{k} \right) \left(\gamma^0 (p^0 + \pi / \beta) + \vec{\gamma} \cdot (\vec{k} + \vec{p}) \right) \right]}{\left(\frac{\pi^2}{\beta^2} + \vec{k}^2 \right) \left[\left(\frac{\pi}{\beta} + p^0 \right)^2 + (\vec{k} + \vec{p})^2 \right]}, \quad (7.6)$$

if we keep only the first term in the sum, where $\omega_0 = \pi/\beta$. As a next step we drop p^0 , so that we have

$$\Pi(\vec{p}, 0) = \frac{g^2}{2\beta} \text{Tr} \int \frac{d^3k}{(2\pi)^3} \frac{\left[\left(\gamma^0 \pi / \beta + \vec{\gamma} \cdot \vec{k} \right) \left(\gamma^0 \pi / \beta + \vec{\gamma} \cdot (\vec{k} + \vec{p}) \right) \right]}{\left(\left(\frac{\pi}{\beta} \right)^2 + \vec{k}^2 \right) \left[\left(\frac{\pi}{\beta} \right)^2 + (\vec{k} + \vec{p})^2 \right]}. \quad (7.7)$$

We then take \vec{p} along the z axis and write $\Pi(p_z) = \Pi(\vec{p}, 0)$. We define

$$C(z) = \int dp_z e^{ip_z z} \Pi(p_z). \quad (7.8)$$

In our calculation we replace $g^2/2\beta$ by unity and use a sharp cutoff so that $|\vec{k}| < k_{max}$.

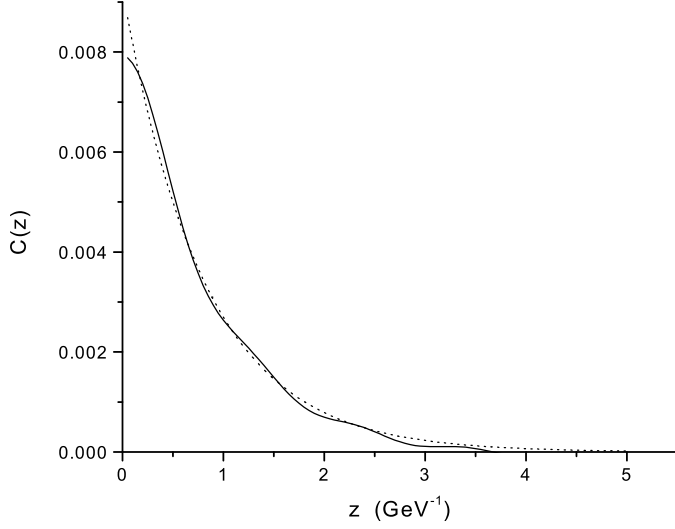


Fig. 18 The function $C(z)$ is shown for a sharp cutoff of $k_{max} = 0.1$ GeV. The dotted line represents an exponential fit to the curve using $m_{sc} = 1.23$ GeV. (We recall that πT is equal to 1.27 GeV.)

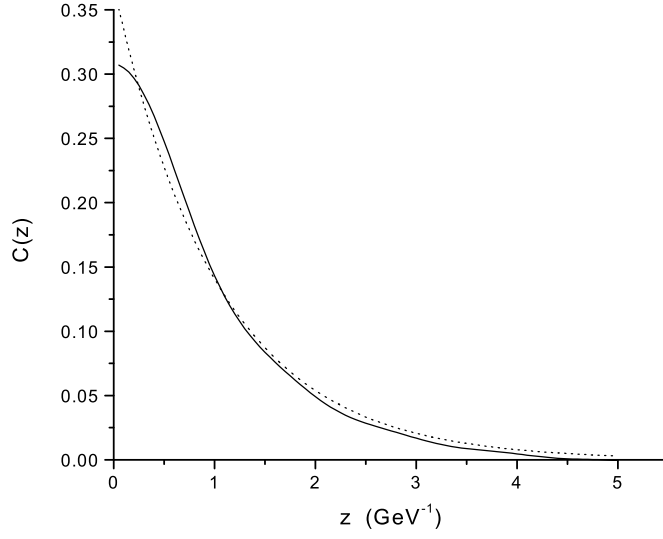


Fig. 19 The function $C(z)$ of is shown for a sharp cutoff of $k_{max} = 0.4$ GeV. The dotted line represents an exponential fit to the curve using $m_{sc} = 0.961$ GeV. (We recall that πT is equal to 1.27 GeV.)